

Visible Surface-Assisted Laser Desorption/Ionization Mass Spectrometry of Small Macromolecules Deposited on the Graphite Plate

Junghwan Kim, Kyungsoo Paek, and Weekyung Kang*

Department of Chemistry, Soongsil University, Seoul 156-743, Korea

Received November 22, 2001

Visible surface-assisted desorption/ionization mass spectrometry (SALDI-MS) has been investigated for several small macromolecules deposited on the graphite plate using laser radiation at 532 nm where most of the macromolecules are transparent. The graphite surface functioned well as a photon absorbing material and an energy transfer mediator for visible light. The results show that visible SALDI is a much softer ionization technique than UV-MALDI and FAB-MS in our results with synthetic macromolecules, PPG, PPGMBE and cavitand molecules. For the SALDI of biomolecules, glycerol as a proton source was essential with the graphite plate. As in visible SALDI, the role division of the photon absorbing material and the cationization agent can provide a generality in mass spectrometric analysis of macromolecules compared with MALDI using the dual functional matrix.

Keywords : SALDI, MALDI, Visible, Graphite, Glycerol.

Introduction

Laser desorption/ionization (LDI) is one of the powerful and well-proven methods in mass spectrometry. The key process in LDI is the rapid dissipation of energy followed by vaporization and formation of charged particles in a small volume. If a matrix is used as a photon absorbing mediator, the ionization technique is called matrix-assisted LDI (MALDI)¹ and has become much more "soft". The UV lasers are almost exclusively used for MALDI based on the strong electronic absorption of aromatic matrices,² and several applications of IR lasers have appeared in the vibrational excitation of hydroxylated viscous molecules such as glycerol.³ Although general criteria for selecting good MALDI matrices have been presented,⁴ it is impossible to predict *a priori* if a compound will form a homogeneous solid solution with an analyte molecule.⁵ This difficulty has meant that the discovery of new matrix materials with desirable properties has been a matter of trial-and-error experimentation.

Most macromolecules have considerable absorption in the UV and IR regions, and the direct absorption of UV and IR laser radiation by analyte molecules can lead to dissociation of weak bonds in many macromolecules, making it difficult to observe the molecular ion.⁶ In spite of the general transparency of most macromolecules in the visible region, the visible LDI has attracted little attention due to the lack of an effective matrix. Only preliminary studies have been reported on the possibilities of visible MALDI using dye molecules, such as Rhodamine 6G and Neutral Red, as matrices.⁷ The visible wavelength laser beam from a tunable dye laser had been used to desorb the macromolecules by heating the underlying copper substrate surface.⁸ The repro-

ducibility of ionization was, however, reported to be a problem in these experiments.

Recently, several researchers have been interested in surface-assisted laser desorption/ionization (SALDI) using graphite as a photon-absorbing material and substrate, to overcome some difficulties of homogeneous sample preparation in MALDI.⁹⁻¹¹ A graphite plate is also a solid material with absorption properties close to those of an ideal black-body, and has a large surface area with potential for rapid heat conduction to analytes. Thus graphite may have a great potential as a photon absorbing material and an energy transfer mediator for SALDI also when a visible laser is used for desorption and ionization of macromolecules.

In this paper, we will demonstrate the LDI time-of-flight mass spectra of synthetic macromolecules and biomolecules deposited on the graphite plate using a 532 nm laser and try to examine the capabilities of visible SALDI in application to mass spectrometric analysis of macromolecules on a solid surface.

Experimental Section

Instrumentation. A home-built 1.0 m linear TOF mass spectrometer was used, a full description of which can be found elsewhere.⁶ The typical background pressure in the vacuum chamber during the operation was 1×10^{-7} torr, using a 4"-diffusion pump (VHS-4, Varian) for a source region and a turbo molecular pump (V 250, Varian) for a drift tube. The graphite plate was mounted on the repelling plate, which was normally maintained at 20 kV, and 25 mm from the gridless and grounded extraction plate with a 15 mm hole in a diameter. A circular (25 mm diameter) dual micro-channel plate (MCP, Galileo Electro-Optics) was used to detect ions. The ion signals were digitized using a LeCroy 9354AL (500 MHz) digital oscilloscope, and the spectra were transferred to an IBM compatible PC for mass calib-

*To whom corresponding should be addressed. Tel: +82-2-820-0438; Fax: +82-2-824-4383; e-mail: wkang@saint.soongsil.ac.kr

ration and data processing. The laser source was a second harmonics of a Nd:YAG laser system (Minilite II, Continuum), with a pulse width of 5 ns and a maximum output energy of 50 mJ. The laser beam was irradiated on the sample plate at an angle of 45°. The power of the laser was attenuated using a neutral density filter.

Sample preparation. The graphite plate (2 mm thickness) for lubrication and machining purposes was used without any treatment unless otherwise noted. If required, the graphite plate was washed in de-ionized water for 1 hour using a sonicator to remove water-soluble metal salts contained and then dried in an oven at 120 °C. Polypropylene glycol (PPG) and PPG monobutylether (PPGMBE) were purchased from Aldrich Co (Milwaukee, WI, USA). Bradykinin, substance P, insulin and glycerol were from Sigma Co (St. Louis, MO, USA). Cavitand was synthesized using the reported procedure.¹² All chemicals were used with no further purification as purchased.

For the analysis of synthetic polymers, 2-3 μL of PPG and PPGMBE solutions (1 mg/mL in CH_3CN) mixed with an aqueous NaCl solution (1 mg/mL) were deposited on the washed graphite plate and then air-dried. Bradykinin, substance P and insulin solutions (0.5 mg/mL) were prepared using 50% CH_3CN aqueous solution. 2-3 μL of each sample was deposited on the graphite plate, and glycerol was dropped on a dried sample spot. The cavitand solution (1 mg/mL in THF) mixed with the CF_3COONa solution (1 mg/mL) was deposited on the washed graphite plate. In all the spectra presented here, 20-30 laser shots were summed to improve the signal-to-noise ratio.

Results and Discussion

Figure 1 shows (a) the visible SALDI spectrum at 532 nm and (b) the UV-MALDI spectrum at 266 nm of PPG 2000

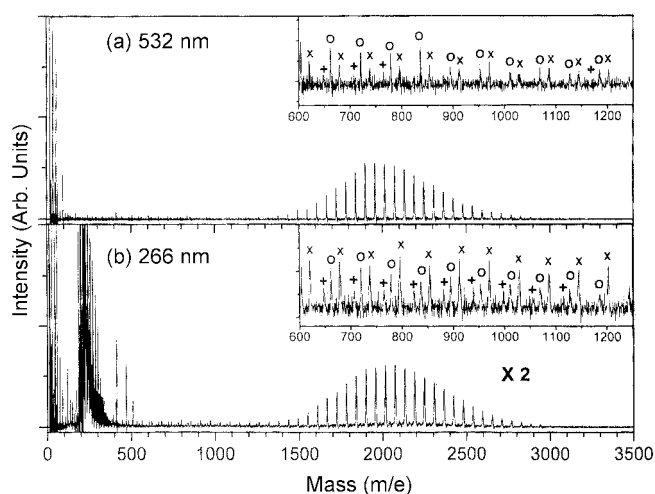


Figure 1. (a) Visible-SALDI and (b) UV-MALDI mass spectrum of PPG 2000 deposited on graphite plate using 532 nm and 266 nm laser radiation, respectively. In UV-MALDI, dithranol was used as a matrix. Symbols, x, + and o denoted in expanded insets represent $58n+69$, $58n+81$ and $58n+97$ mass series of the fragment ion, respectively.

sampled on the graphite plate using NaCl salt as a cationization agent. Both spectra were obtained at the optimized conditions. When the graphite plate was used as a sample support, the ion signals were more intense and had a better signal-to-noise ratio than when the metal plate was used, also in UV-MALDI spectrum using dithranol as a matrix. In addition, evaporation by smearing the sample solution into the graphite plate can prevent a heterogeneous concentration in a round rim of the sample spot caused by the spread of the solution on the metal surface. The mass series of dominant ion signals observed was $58n + 41$ ($n = 20-50$), which is consistent with that of the sodiated PPG molecule, $\text{HO}(-\text{C}_3\text{H}_6\text{O})_n\text{-H} \cdot \text{Na}^+$. The calculated number-averaged molecular weight is 2060 in visible SALDI, which is slightly larger than 2020 in UV-MALDI. Comparison of the two spectra has not shown a large difference in the main ion signals except for a more intense ion signal and a slightly larger average molecular weight in visible SALDI. However, there are some large differences between the two spectra in the low mass region. The first one is the congestion effect in the low mass region. In Figure 1(b) obtained at 266 nm, the spectrum shows a number of intense peaks in the mass range of 200-400 due to the high photon energy directly absorbed. These are assigned to the adduct ions of dithranol used as a matrix and the hydrogenated carbon cluster ions originating from the graphite plate. These very intense ion peaks in the low mass region cause a weakening of the higher mass ion signals by saturation of the MCP detector,¹³ and low mass congestion prohibits structural analysis based on the fragmentation pattern and a study on the reaction mechanism. However, the congestion does not take place in the visible SALDI spectrum of PPG 2000.

The ion signals shown in the mass region of 500-1200 amu of Figure 1 are interpreted as ions to be fragmented during ionization or desorption. They consist of three mass series, the $58n + 69$, the $58n + 81$ and the $58n + 97$ series ($n = 7-20$), which are well consistent with the results of Donovan under delayed extraction mode.¹⁴ The insets of Figure 1 show that the fragmented ion signals are more intense when a UV laser is used, despite the more intense PPG ion signals in visible SALDI. This low fragmentation implies that the visible SALDI technique is a much milder ionization process than UV-MALDI.

The ion intensities and the resolution of the PPG 2000 molecular ion have been determined as a function of the laser fluence, and the results are plotted in Figure 2 on the log/log graph for ion intensity and on the linear/linear graph for resolution. At low laser power, the UV laser generates more intense ion signals than the visible laser. However, when the visible laser was used for desorption and ionization of PPG 2000 molecules, the ion signals increased more steeply as the laser pulse energy was increased, reaching saturation at about 2.0 MW/cm^2 . The saturation of the curves at high laser fluences results most likely from the onset of secondary processes such as an increased number of collisions in the expanding particle plume and from charge repulsion. The saturation correlates directly with the deterio-

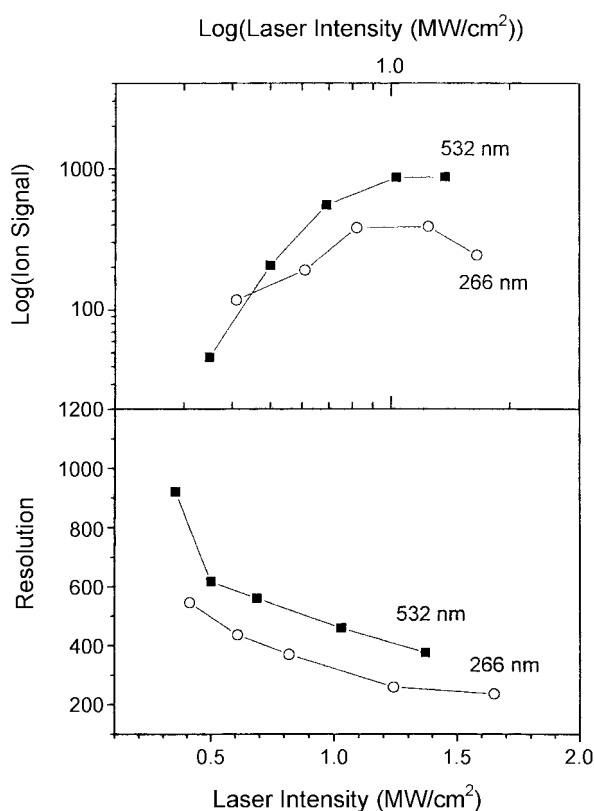


Figure 2. The intensity and resolution of PPG molecular ion peaks as function of laser fluence in visible SALDI (filled square) and UV-MALDI (filled circle) mass spectra.

ration of the mass spectra, *i.e.* with broadening and distortion of signal peaks at these fluences and with increased fragmentation. The initial slopes of the lines at lower laser fluence before saturation in Figure 2 (a) are approximately 3.7 for 532 nm and 1.8 for 266 nm. The slope in the log-log plot of intensity vs laser fluence represents the number of photons absorbed in the determining step of the multiphoton process. The ratio of slopes is very consistent with the inverse of the ratio of photon energy at 532 nm and 266 nm.

The ion signals of PPG2000 by the UV laser decreased after reaching saturation, and the resolution was lowered when the laser fluence was increased, and fragmentation in the 600-1200 amu region increased. As a result of increased fragmentation, a significant shift in the number of oligomers in its length was induced from 35 to 32 with the maximum intensity in the position of apparent molecular weight distribution, and the normal Gaussian distribution distorted into an asymmetrical shape with slightly higher abundance in the shorter oligomer length. This indicates that the molecule with a longer chain length is more easily fragmented, and this unequal fragmentation according to chain length may result in a significant disturbance in determining the molecular weight distribution of synthetic polymers. The dramatic mass discrimination effect is shown in Figure 3 of mass spectrum of PPGMBE. The TOF mass spectra of PPGMBE 4000 have three unique distributions of ion peaks. One of them shows a broad non-Gaussian distribution in the mass

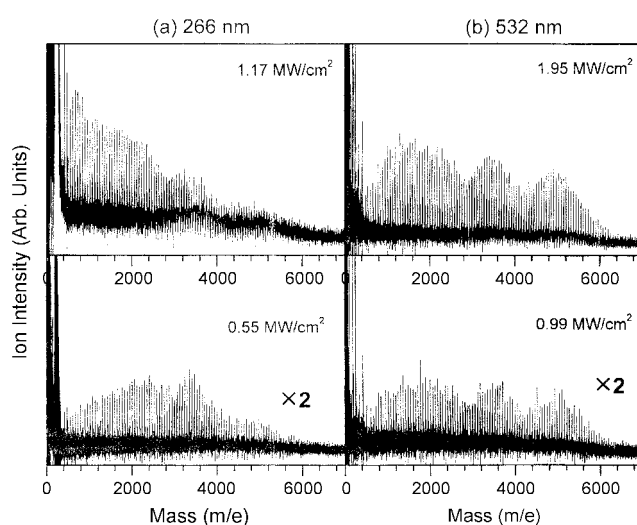
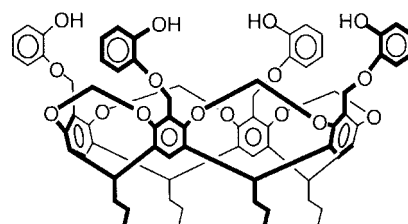


Figure 3. SALDI mass spectra of PPGMBE molecules deposited on the graphite plate to variation of laser fluence of (a) 532 nm and (b) 266 nm laser radiation.

range of 500-4000 amu, and the others show bimodal Gaussian distributions convoluted in the range of 2500-4500 amu and 3500-6500 amu. The ion peaks with the Gaussian distribution are assigned to $58n + 97$ ($n = 30-110$), which is very consistent with sodiated PPGMBE molecule, $\text{HO}-(\text{C}_3\text{H}_6\text{O})_n-\text{C}_4\text{H}_9 \cdot \text{Na}^+$. However, the mass series of the non-Gaussian distribution is $58n + 81$ ($n = 7-70$), which is supposed to be a fragmented ion peak. While the intensity ratios among these three mass series do not show large differences according to the variation of laser fluences in visible TOF mass spectra, they have large differences in UV TOF mass spectra as shown in Figure 3. When the UV laser was used to desorb and ionize the PPGMBE molecule, the mass series of the second Gaussian distribution in the mass range of 3500-6000 amu was less abundant than the first Gaussian mass distribution even at the low laser fluence. As the laser fluence was increased, the ion peaks with higher mass series rapidly decreased accompanying the increase of fragmented ion signals in the mass range of 500-2000 amu and could hardly be observed at laser fluence above 1.17 MW/cm². The mass-dependent fragmentation by the UV laser might result from a higher degree of relaxation of excess energy by higher photon energy than with the visible laser, and this mass discrimination effect is one of the barriers to determining the average molecular weight of synthetic polymer with disperse distribution using a mass spectrometer.



Tetrakis(catecholy)methylcavitand

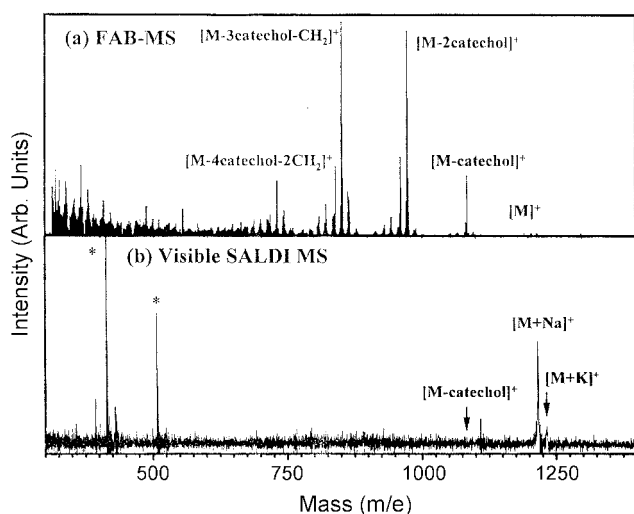


Figure 4. (a) FAB-MS and (b) Visible-SALDI mass spectrum of tetrakis(catecholylmethyl) cavitaand. The peaks marked with an asterisk originated from diffusion pump oil.

The use of mass spectrometry in the study of host-guest complexation and molecular recognition has been an enormously active area of research over the last decade.¹⁵⁻¹⁷ Most host molecules, such as calixarene and cavitaand, have a high molecular weight and have various moieties that can be easily fragmented in vaporization and ionization.¹⁸ To examine the capability of the visible SALDI in the analysis of supramolecules, we compared the visible SALDI with fast-atom-bombardment mass spectrometry (FAB-MS), which is known to be one of the mildest ionization methods. Figure 4 depicts the mass spectra of tetrakis(catecholylmethyl)-cavitaand, which has an interesting size and shape selectivity toward various diamines.¹⁹ The FAB mass spectrum of this cavitaand shows only the fragmented ion peaks. The dominant peaks among them are assigned to the mass series of fragments that catechol units split out from molecular ions. However, in the visible SALDI spectrum, the sodiated molecular ion peak is clearly observed without showing fragmentation, indicating that the visible SALDI technique is at least as mild as the FAB-MS.

The key point as to be considered as the vaporization, *i.e.* desorption, is the ionization in mass spectrometric analysis of macromolecules. Pseudo-molecular ions of an attached ion form with metal ions or protons are usually observed rather than the molecular ions by direct ionization. The matrix in MALDI for analysis of biomolecules is believed to serve two major functions: as the energy transfer mediator of photon energy and as the proton source for assisted ionization. Thus, proton affinity in the excited state as well as photophysical properties is also one of the important parameters when selecting an adequate matrix for a given biomolecular analyte.²⁰ In SALDI using a graphite plate as the photon absorbing material, the analytes are not easily protonated because there is no matrix as the proton source. Homogeneous sample preparation is also not easy for hydrophilic biomolecules as synthetic polymers due to the

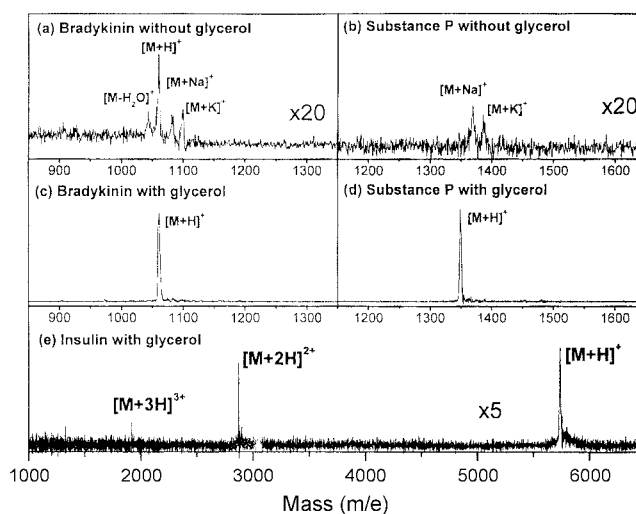


Figure 5. Visible SALDI mass spectra of bradykinin, substance P and insulin molecules. (a) and (b) were obtained using no any cationization agent and were smoothed to improve the signal-to-noise ratio. For (c), (d) and (e), glycerol was used as protonation agent.

hygroscopic surface of graphite. Figure 5 (a) and (b) show the visible SALDI spectra of bradykinin and substance P, which are the prototypes of biomolecules in mass spectrometric analysis, obtained without any cationization agent. As shown in the spectra, the pseudo-molecular ion signals were short-lived and were very weak as to be barely observed after smoothing. This is consistent with Sunner's result in UV-SALDI using graphite powder and an N₂ laser without glycerol.⁹ The sodiated and potassiated ion peaks may originate from impurities existing on an untreated graphite plate. However, when the peptides were prepared with glycerol, which is a highly viscous proton source, the protonated ion peaks were much higher as shown in Figure 5 (c) and (d). In addition, the ion signals were very long-lived as compared with when glycerol was absent. To confirm that both glycerol and graphite are essential in obtaining visible SALDI spectra, we conducted another control experiment. we observed neither glycerol nor peptide spectra with a glycerol solution, only on the aluminum probe, *i.e.* in the absence of graphite. Figure 5 (e) depicts the visible SALDI spectrum of insulin. The molecular ion signal is clearly detected with multiply charged ions, [M+2H]²⁺ and [M+3H]³⁺, when prepared with glycerol. Glycerol was initially used as a liquid matrix in IR-MALDI because it has a strong absorption band in the IR, near 3 μm.²¹ While glycerol must be responsible for both photon absorption and the assisted-ionization in IR-MALDI, it is only responsible as the proton source in visible SALDI because of its transparency to visible light.

In conclusion, we have demonstrated that the LDI spectra of small macromolecules, synthetic polymers and biomolecules can be obtained using a graphite plate and a visible laser. The use of a visible laser can prohibit the direct photon absorption of analytes due to transparency for most of macromolecules in the LDI mass spectrometric technique.

As in SALDI, the role division of the photon absorbing material and the cationization agent provides a generality in mass spectrometric analysis of macromolecules compared with MALDI using the dual functional matrix. We are continuing to study the region of the applications of the visible SALDI.

Acknowledgment. This paper is dedicated to K.-H. Jung on the occasion of his 65th anniversary. This research was financially supported by the Korean Research Foundation (BK21 program), which is gratefully acknowledged.

References

1. Karas, M.; Bachmann, D.; Bahr, U.; Hillenkamp, H. *Int. J. Mass Spectrom. Ion Processes* **1987**, *78*, 53.
2. Krause, J.; Stoeckli, M.; Schunegger, U. R. *Rapid Commun. Mass Spectrom.* **1996**, *10*, 1927.
3. Menzel, C.; Berkenkamp, S.; Hillenkamp, F. *Rapid Commun. Mass Spectrom.* **1999**, *13*, 26.
4. Hillenkamp, F.; Karas, M.; Beavis, R. C.; Chait, B. T. *Anal. Chem.* **1991**, *63*, 1193A.
5. Allwood, D. A.; Perera, I. K.; Perkins, J.; Dyer, P. E.; Oldershaw, G. *Appl. Surf. Sci.* **1996**, *103*, 231.
6. Kang, W. K.; Kim, J.; Paek, K.; Shin, K. S. *Rapid Commun. Mass Spectrom.* **2001**, *15*, 941.
7. (a) Smith, C. J.; Chang, S. Y.; Yeung, E. S. *J. Mass Spectrom.* **1995**, *30*, 1765 (b) Cornett, D. S.; Duncan, M. A.; Amster, I. J. *Anal. Chem.* **1993**, *65*, 2608.
8. Schieltz, D. M.; Chou, C. W.; Luo, C. W.; Thomas, R. M.; Williams, P. *Rapid Commun. Mass Spectrom.* **1992**, *6*, 631
9. (a) Sunner, J.; Dratz, E.; Chen, Y.-C. *Anal. Chem.* **1995**, *67*, 4335 (b) Michael, J. D.; Knochenmuss, R.; Zenobi, R. *Anal. Chem.* **1996**, *68*, 3321.
10. Kim, J.; Kang, W. K. *Bull. Korean Chem. Soc.* **2000**, *21*, 401.
11. Kim, H.-J.; Lee, J.-K.; Park, S.-J.; Ro, H. W.; Yoo, D. Y.; Yoon, D. Y. *Anal. Chem.* **2000**, *22*, 5673.
12. Ihm, C.; Kim, M.; Ihm, H.; Paek, K. *J. Chem. Soc. Perkin Trans. 2* **1999**, 1569.
13. David, C. S.; Liang, L. *Anal. Chem.* **1997**, *69*, 4176.
14. Mowat, I. A.; Donovan, R. J.; Maier, R. J. *Rapid Commun. Mass Spectrom.* **1997**, *11*, 89.
15. Vincenti, M. *J. Mass Spectrom.* **1995**, *30*, 925.
16. Przybylski, M.; Glocker, M. O. *Angew. Chem. Int. Ed. Engl.* **1996**, *35*, 806.
17. Schalley, C. A. *Int. J. Mass Spectrom.* **2000**, *194*, 11.
18. (a) Gutsche, C. D. *Calixarenes, Monographs in Supramolecular Chemistry*; Stoddart, J. F., Ed.; The Royal Society of Chemistry Press: Cambridge, 1989; Vol. 1. (b) Cram, D. J. *Science* **1988**, *219*, 1177.
19. Lee, H.-J.; Paek, K. *Bull. Korean Chem. Soc.* **2000**, *21*, 526.
20. Krause, J.; Stoeckli, M.; Schunegger, U. P. *Rapid Commun. Mass Spectrom.* **1996**, *10*, 1927.
21. Tanaka, K.; Waki, H.; Idao, Y.; Akita, S.; Yoshida, Y.; Yoshida, T. *Rapid Commun. Mass Spectrom.* **1988**, *2*, 151.